Protein expression of nucleophosmin, annexin A3 and nm23-H1 correlates with human nasopharyngeal carcinoma radioresistance *in vivo*

SONG QU[1,2], XIAO-YU LI[1,2], ZHONG-GUO LIANG[1,2], LING LI[1,2], SHI-TING HUANG[1,2], JIA-QUAN LI[2,3], DAN-RONG LI[2,3] and XIAO-DONG ZHU[1,2]

[1]Department of Radiation Oncology, The Affiliated Tumor Hospital of Guangxi Medical University, Cancer Institute of Guangxi Zhuang Autonomous Region;
[2]Guangxi Key Laboratory of Early Prevention and Treatment for Regional High Frequency Tumor;
[3]Guangxi Medical Scientific Research Center, Guangxi Medical University, Nanning, Guangxi 530021, P.R. China

Received January 14, 2015; Accepted February 11, 2016

DOI: 10.3892/ol.2016.4632

Abstract. Radioresistance is a significant obstacle in the treatment of endemic nasopharyngeal carcinoma (NPC). The present study aimed to identify proteins associated with radioresistance in NPC *in vitro* and *in vivo*. Proteomics analyses were conducted to screen for differentially-expressed proteins (DEPs) in parental CNE-2 cells and CNE-2R cells. Using proteomics approaches, 16 DEPs were identified. Of these DEPs, nucleophosmin (NPM1), annexin A3 and nm23-H1, were verified using western blot analyses. The tumorigenicity was investigated using mouse xenograft tumorigenicity assays, and tumor growth curves were generated. The protein expression of NPM1, annexin A3 and nm23-H1 was examined by immunohistochemically staining tumor tissues. NPM1 and annexin A3 protein levels were downregulated in the CNE-2R cells, whereas nm23-H1 expression was upregulated. *In vivo* tests showed that compared with the CNE-2 tumors, CNE-2R tumor growth was significantly retarded ($P<0.05$). CNE-2 tumor progression was inhibited by irradiation, but CNE-2R tumor progression was not, indicating that the CNE-2R cells were also radioresistant *in vivo*. NPM1 and annexin A3 expression was significantly lower in non-irradiated (NIR)-CNE-2R tumors compared with NIR-CNE-2 tumors ($P<0.01$). However, Nm23-H1 protein levels were significantly higher ($P<0.05$). Overall, the present study established comparable radioresistant and radiosensitive tumor models of human NPC, and identified candidate biomarkers that may correlate with radioresistance. The data showed that dysregulation of NPM1, annexin A3 and nm23-H1 expression correlated with the cellular and tumor radioresponse. These proteins are involved in the regulation of intracellular functions, including stress responses, cell proliferation and DNA repair. However, further clinical evaluations are required.

Correspondence to: Professor Xiao-Dong Zhu, Department of Radiation Oncology, The Affiliated Tumor Hospital of Guangxi Medical University, Cancer Institute of Guangxi Zhuang Autonomous Region, 71 He Di Road, Nanning, Guangxi 530021, P.R. China
E-mail: zhuxdonggxmu@126.com

Key words: nasopharyngeal neoplasms, radioresistance, protein expression, animal model, xenograft

Introduction

Nasopharyngeal carcinoma (NPC) is an endemic disease in Southeast Asia and Southeast China. Radiotherapy is the primary treatment for patients with non-metastatic NPC, and concurrent chemoradiotherapy is considered the standard treatment for locally-advanced NPC (1,2). Due to radioresistance, certain patients with NPC present with local recurrences and distant metastases 1-2 years after treatment (3). The primary reason for the failure to respond to radiotherapy is radioresistance. Numerous studies have aimed to identify differentially-expressed proteins (DEPs) associated with cancer radioresistance between paired parental cell lines and radioresistant subclones using high-throughput proteomics methods. These studies focused either on paired parental and radioresistant cancer cells or immunochemical analyses of tissues from patients with locoregional failure. These methods have limitations in the screening for novel biomarkers that can be used for diagnosis and treatment. Nevertheless, there was no overlap in the proteins involved in radioresistance in the various studies. This may be due to distinct tissue specificity or the different methods used. Although several radioresistant subclones of NPC have been established (3,4), no animal experiments have been reported thus far. As described previously (3), we have also established a subclone (CNE-2R) by exposing CNE-2 cells to a cumulative radiation dose of 64 Gy. CNE-2R and CNE-2 cells have a different survival fraction at 2 Gy value, as well as varying α, β and α/β values, which were verified by colony formation assays and complementary (c)DNA microarray analyses (3). A study by Sekhar *et al* found that the inhibition of DNA repair due to the inhibition of nucleophosmin (NPM) shuttling increases the efficacy of

DNA-damaging therapeutic strategies (5), thereby increasing radiosensitivity. In another study, annexin A3 was selected as a protein of interest in paired prostate cancer cell lines, and five regulated proteins (nucleoside diphosphate kinase A, heat shock 70-kDa protein 8, DNA-(apurinic or apyrimidinic site) lyase, plasminogen activator inhibitor 1 RNA-binding protein and Ras-related protein Rab-11A) were validated using western blot analyses. However, annexin A3 was not validated (6). Nm23-H1 was first identified as a biological predictor of radioresistance based on cDNA array and proteomics analyses (7). However, it remains unclear as to whether it acts as a biomarker.

In the present study, changes in protein expression associated with radioresistance were investigated. First, possible DEPs for NPC radioresistance were identified by comparing CNE-2R cells and parental CNE-2 cells *in vitro*. Next, three particularly significant DEPs, NPM1, annexin A3 and nm23-H1, were validated using western blot assays (8). Comparable radioresistant and radiosensitive tumor models of NPC were established by subcutaneously injecting CNE-2R cells and CNE-2 cells into athymic nude mice. The xenografts were irradiated with fractioned X-ray irradiation and the growth characterization was studied. Finally, in order to validate the expression of these proteins *in vivo*, NPM1, annexin A3 and nm23-H1 protein expression was immunohistochemically examined in the tumor tissues. The findings indicated that NPM1, annexin A3 and nm23-H1 are potential biomarkers for predicting the response of NPC to radiotherapy.

Materials and methods

Cell lines and cell culture. Poorly-differentiated human NPC CNE-2 cells were purchased from the Cancer Hospital of Fudan University (Shangha, China). CNE-2R cells were induced by treating the parental CNE-2 cells with fractioned cobalt-60 γ-ray irradiation (total dose, 6,400 cGy; Theratron 780; Theratronics International Ltd., Kanata, Canada) (3). The CNE-2R and CNE-2 cells were cultured separately in RPMI 1640 medium (Hyclone; GE Healthcare Life Sciences, Logan UT, USA) supplemented with 10% fetal bovine serum (Hangzhou Sijiqing Biological Engineering Materials Co., Ltd., Hangzhou, China), penicillin G (100 kU/l; (North China Pharmaceutical Co., Ltd., Shijiazhuang, China) and streptomycin (100 mg/l; Qilu Pharmaceutical Co., Ltd., Jinan, China). The cells were maintained at 37˚C in a 5% CO_2 incubator until use.

Xenograft tumorigenicity assays. BALB/c athymic nude mice (males and females, aged 4-6 weeks; n=36) were obtained from the Animal Laboratory Center of Guangxi Medical University [Guangxi, China; license number, SCXK (Gui) 2009-002]. The mice were housed five per cage, and maintained under specific pathogen-free conditions. The mice were randomly divided into three groups of 12 animals each: Group A, treated with CNE-2R cells; group B, treated with CNE-2 cells; and group C, treated with saline. In group A, CNE-2R cells ($1x10^7$ in a total volume of 0.2 ml) were subcutaneously injected into the right hind legs of 6 mice, and both the right and left hind legs of 6 mice. In group B, CNE-2 cells ($1x10^7$ in a total volume of 0.2 ml) were subcutaneously injected into the right hind legs of 6 mice, and both the right and left hind legs of 6 mice. The subcutaneous xenograft tumors were palpated and the diameters measured every other day using calipers. The volumes of the tumors were calculated using the following formula: Volume = 0.5 x length (cm) x $width^2$ (cm). Next, a growth curve of the two tumors group was generated. Tumor doubling times (DTs) were calculated using the following formula: $DT = \ln(2Dt) / \ln(V_2 / V_1)$, where V_1 and V_2 are the volume estimates in each scan obtained D*t* days apart (9). Tumor-bearing mice received X-ray irradiation when the tumors reached ~1 cm in the longest diameter (13 days after cancer cell implantation). The mice received 16 Gy in 4 fractions delivered over 8 days. Local external beam radiation was applied (6-MV X-rays at a dose rate of 400 MU/min) using a clinical X-ray therapy unit (Precise Elekta; Eleckta, Stockholm, Sweden). Right-sided tumors were locally irradiated, with the rest of the body protected from irradiation with lead shielding. Single posteroanterior external beam radiation fields were used. Irradiated (IR) and non-IR (NIR) groups were created. All animal experiments were performed in accordance with Guangxi Medical University Ethics Committee guidelines.

Hematoxylin and eosin (H&E) staining. The mice were sacrificed 2 weeks after irradiation, and autopsies were performed on all injected mice. Xenograft tumors were excised, immediately placed in 10% neutral-buffered formalin and fixed for 24-48 h. Subsequent to fixation, samples were dehydrated and embedded in paraffin. A series of 4-μm sections were prepared from each specimen, mounted on poly-lysine-coated glass slides and dried for 4-5 h at 37˚C to promote adhesion. H&E staining was performed on one section from each specimen.

Tumor tissue immunohistochemistry. Immunohistochemical staining of the paraffin sections was performed after dewaxing and rehydrating the sections. Briefly, 4-μm tissue sections were blocked with 3% hydrogen peroxide for 10 min to inactivate endogenous peroxidase activity. Once the tissue sections had been autoclaved at 120˚C for 10 min in an antigen retrieval solution [10 mmol/l sodium citrate buffer (pH 6.0)], they were incubated overnight at 4˚C with a polyclonal rabbit NPM1 antibody (cat. no. 10306-1-AP; 1:100 dilution; ProteinTech Group, Inc., Chicago, IL, USA), a polyclonal rabbit anti-annexin A3 (cat. no. ab33068; 1:100 dilution; Abcam, Cambridge, UK) or a monoclonal rabbit nm23-H1 (cat. no. 7948-1; 1:100 dilution; Epitomics, Inc., Burlingame, CA, USA) antibodies. The sections were then incubated with Biotin-conjugated Affinipure goat anti-rabbit immunoglobulin G(H+L) (cat. no. SA00004-2; 1:200 dilution; ProteinTech Group, Inc.) for 1 h at room temperature, followed by incubation with the streptavidin-biotin complex (cat. no. SA00001-0; 1:200 dilution; ProteinTech Group, Inc.). The color was developed after incubation for 3-5 min with 3,3'-diaminobenzidine solution (0.05%). The sections were then counterstained with hematoxylin and mounted. For the negative controls, the primary antibodies were replaced with phosphate-buffered saline. The sections were observed using light microscopy. The degree of NPM1 protein expression was assessed based on the percentage of positive cells, whereas annexin A3 and nm23-H1 expression were quantified using a computer-based quantitative color

Table I. NPM1 protein expression in xenograft tumor tissues.

Tumors	NPM1, %
NIR-CNE-2	56.3±5.2[a]
NIR-CNE-2R	36.0±4.2[b]
IR-CNE-2	35.3±5.5[c]
IR-CNE-2R	36.3±4.7

[a]P<0.01 vs. NIR-CNE2R and IR-CNE-2; [b]P>0.05 vs. IR-CNE-2R; [c]P>0.05 vs. IR-CNE-2R. NPM1, nucleophosmin; IR, irradiated; NIR, non-irradiated.

Table II. MOD of annexin A3 protein in xenograft tumor tissues.

Tumors	MOD value of annexin A3
NIR-CNE-2	0.062±0.009[a,b]
NIR-CNE-2R	0.035±0.012[c]
IR-CNE-2	0.051±0.009[d]
IR-CNE-2R	0.029±0.007

[a]P<0.01 vs. NIR-CNE-2R; [b]P>0.05 vs. IR-CNE-2; [c]P>0.05 vs. IR-CNE-2R; [d]P<0.01 vs. IR-CNE-2R. MOD, mean optical density; IR, irradiated; NIR, non-irradiated.

Table III. MOD of nm23-H1 protein in xenograft tumor tissues.

Tumors	MOD value of nm23-H1
NIR-CNE-2	0.043±0.007[a,b]
NIR-CNE-2R	0.056±0.007[c]
IR-CNE-2	0.046±0.007[d]
IR-CNE-2R	0.079±0.009

[a]P<0.05 vs. NIR-CNE-2R; [b]P>0.05 vs. IR-CNE-2; [c]P<0.01 vs. IR-CNE-2R; [d]P<0.01 vs. IR-CNE-2R. MOD, mean optical density; IR, irradiated; NIR, non-irradiated.

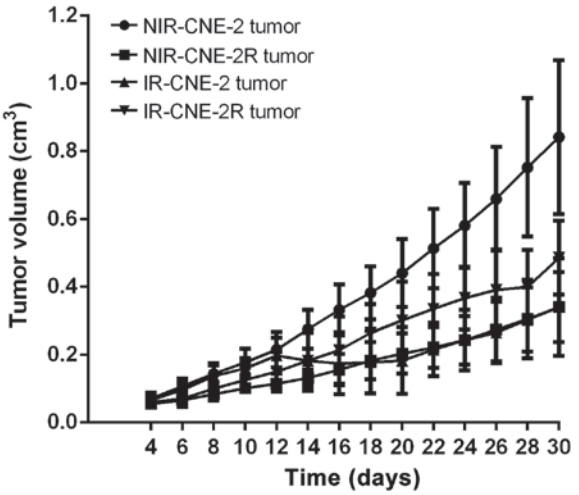

Figure 1. Growth curve of non-irradiated (NIR)-CNE-2R tumors, NIR-CNE-2 tumors, irradiated (IR)-CNE-2R tumors and IR-CNE-2 tumors. The tumor volume doubling times of the NIR-CNE-2R, NIR-CNE-2, IR-CNE-2R and IR-CNE-2 tumors were 4.8, 3.9, 6.2 and 17.1 days, respectively.

image analysis software (Image-Pro Plus 6.0; Media Cybernetics, Bethesda, MD, USA). The mean optical density (MOD) of 10 views was obtained. The relative amounts of annexin A3-positive and nm23-H1-positive cells are expressed as a ratio of the MODs of the CNE-2R and CNE-2 tumors.

Statistical analysis. Data analyses were performed using SPSS version 13.0 (SPSS Inc., Chicago, IL, USA). Differences in protein expression were compared using a one-way analysis of variance. Significance levels were further evaluated using Bonferroni's multiple comparisons tests. All data are expressed as the mean ± standard deviation. P<0.05 was considered to indicate a statistically significant difference.

Results

Tumor growth characterization. The NIR-CNE-2R tumors grew significantly slower than the NIR-CNE-2 tumors (P=0.025). The doubling times of the NIR-CNE-2R and NIR-CNE-2 tumors were 4.8 and 3.9 days, respectively. CNE-2R tumor volume progression was not inhibited by irradiation, whereas CNE-2 tumor volume was inhibited (Fig. 1). The tumor volume doubling times for the IR-CNE-2R and IR-CNE-2 tumors were 6.2 days and 17.1 days, respectively. The volume increase rate of the IR-CNE-2R tumors was higher than that of the IR-CNE-2 tumors.

Histological findings. A large amount of tumor necrosis was observed in the NIR-CNE-2R and NIR-CNE-2 tumors. However, there were only a few scattered necrotic areas observed in the IR-CNE-2R tumors. Following irradiation, extensive degeneration and pyknotic cells were observed in the tumors. Cancer cells were nested, with large nuclei and abundant cytoplasm, and round or oval hyperchromatic nuclei. Keratinization was minimal or absent, and the mitotic rates were variable. The tumor cells possessed morphological characteristics similar to those of human NPC cells.

NPM1, annexin A3 and nm23-H1 immunohistochemical analysis. Immunohistochemical analyses were used to compare NPM1, annexin A3 and nm23-H1 protein expression in the CNE-2 and CNE-2R tumor tissues. For NPM1 immunohistochemistry, positive cells were distinguished by brown staining in the nuclei of the cancer cells (Fig. 2). Annexin A3 and nm23-H1 were predominately expressed in the cytoplasm; therefore, brown granules in the cytoplasm of the carcinoma cells and interstitial cells were considered positive (Figs. 3 and 4). NPM1 and annexin A3 expression was significantly lower in the NIR-CNE-2R tumors compared with that in the NIR-CNE-2 tumors (P=0.007 and P=0.005; Tables I and II), whereas Nm23-H1 expression was significantly higher (P=0.036; Table III). These results are in agreement with results from our previous *in vitro* study (9). Annexin A3 expression was significantly downregulated in the IR-CNE-2R

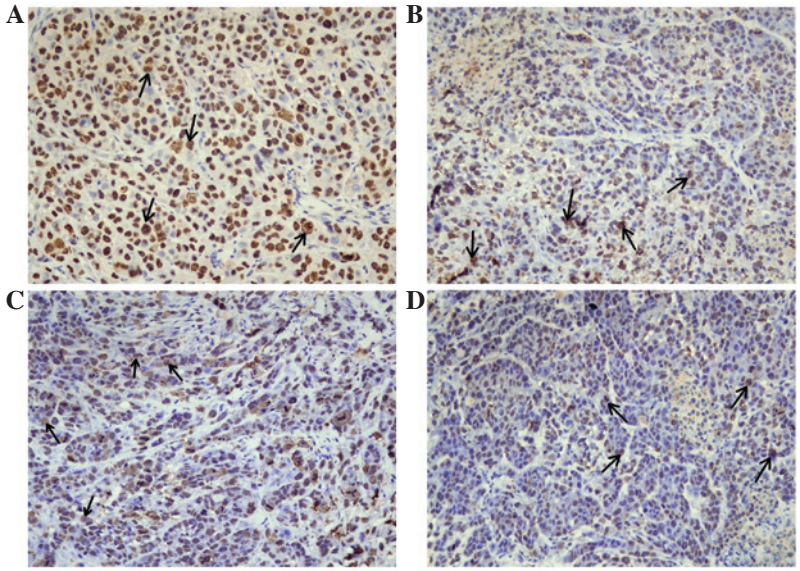

Figure 2. Nucleophospmin expression in different radiosensitive tumors (magnification, x400). (A) Non-irradiated (NI)-CNE-2 tumor, (B) NI-CNE-2R tumor, (C) irradiated (IR)-CNE-2 tumor and (D) IR-CNE-2R tumor. Arrows indicate positive expression in the cell nuclei.

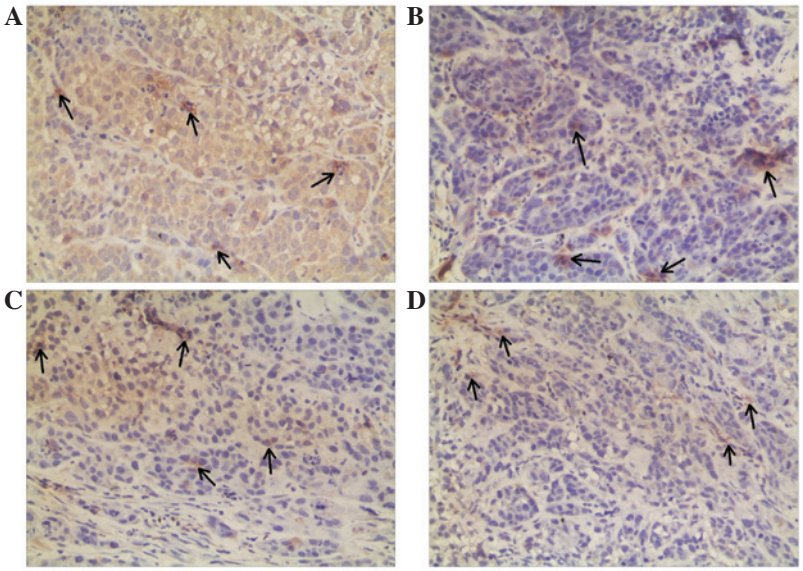

Figure 3. Annexin A3 expression in different radiosensitive tumors (magnification, x400). (A) Non-irradiated (NI)-CNE-2 tumor, (B) NI-CNE-2R tumor, (C) irradiated (IR)-CNE-2 tumor and (D) IR-CNE-2R tumor. Arrows indicate predominant expression in the cytoplasm of the cancer cells.

tumors compared with the IR-CNE-2 tumors (P=0.003; Table II). However, Nm23-H1 protein expression was significantly upregulated (P=0.004; Table III). NPM1 levels were slightly upregulated in the IR-CNE-2R tumors compared with the NIR-CNE-2 tumors; however, the difference was not significant (P=0.731; Table I).

Discussion

Previous studies have screened for DEPs associated with radioresistance in NPC (4,10). One study identified seven upregulated genes in radioresistant subclones of CNE2. Among these, gp96 and growth differentiation factor 15 showed the highest expression (10). Feng *et al* (4) identified 34 DEPs using proteomics methods. It was found that the downregulation of 14-3-3σ and Maspin, and the upregulation of heat shock protein family A (Hsp70) member 5 and manganese superoxide dismutase correlated with NPC radioresistance. However, none of these DEPs were validated *in vivo*.

To identify more reliable markers for radioresistance, a sub-line (termed CNE-2R) was established by exposing CNE-2 cells to a cumulative irradiation dose of 64 Gy (3). In our previous study, proteomic analyses were used to search for potential biomarkers of radioresistance. NPM1, annexin A3 and Nm23-H1 proteins were among the 16 identified DEPs that were regulated more than 2-fold (11). Furthermore, a comparable radioresistant and radiosensitive tumor model of human NPC was established, and the level of these three proteins was compared *in vivo*. The results indicated that

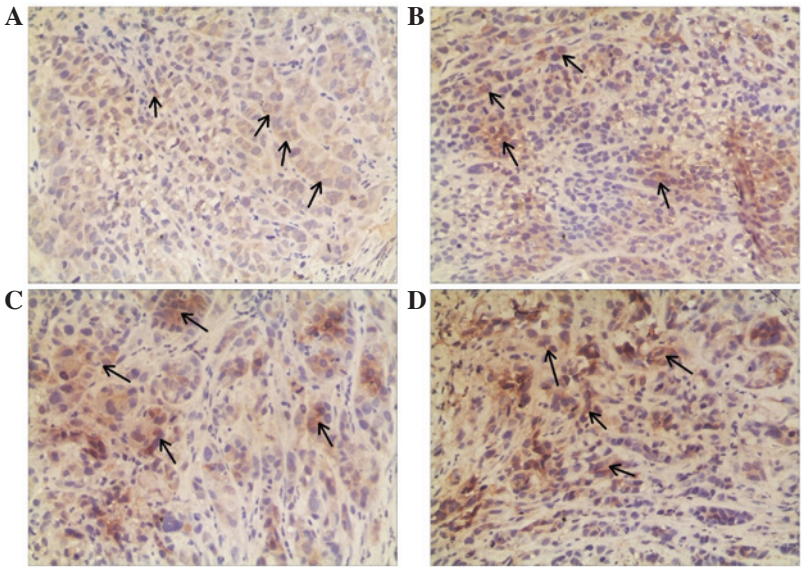

Figure 4. Nm23-H1 expression in different radiosensitive tumors (magnification, x400). (A) Non-irradiated (NI)-CNE-2 tumor, (B) NI-CNE-2R tumor, (C) irradiated (IR)-CNE-2 tumor and (D) IR-CNE-2R tumor. Arrows indicate predominant expression in the cytoplasm of the cancer cells.

NPM1, annexin A3 and Nm23-H1 protein expression likely correlate with NPC radioresistance.

NPM1 (also known as nucleolar phosphoprotein B23) is a molecular chaperone involved in numerous cellular processes, including centrosome duplication, ribosome biogenesis, cell-cycle progression (12) and DNA damage repair (13). Enhanced NPM1 expression causes uncontrolled cell growth. In tumor cells, NPM overexpression is associated with increased cell growth and proliferation. It has been demonstrated that NPM1 protein levels are inversely associated with cell doubling time in human cancer cells (14). Higher NPM expression is associated with local recurrence rate and/or better disease-free survival in certain types of cancers; therefore, it has been proposed that NPM acts as a marker for oral squamous cell carcinomas (15). Loss of NPM expression contributes to tumorigenesis via its interaction with the protein alternate reading frame, thereby controlling genomic stability (16). Recently, the association between NPM expression and DNA repair has been elucidated. Sekhar *et al* (5) demonstrated that the inhibition of DNA repair by NPM shuttling inhibition increased the efficacy of DNA-damaging therapeutic strategies such as ionizing radiation. In the present study, NPM1 protein expression was significantly lower in the CNE-2R cells compared with the CNE-2 cells. *In vivo* tests also showed that NPM1 expression was lower in the NIR-CNE-2R tumors compared with the NIR-CNE-2 tumors. Notably, NPM1 protein expression was slightly higher in the IR-CNE-2R tumors compared with the IR-CNE-2 tumors, which appears paradoxical with NPM1 protein expression levels in non-irradiated tumors. We propose that this may be as the IR-CNE-2R cells have acquired increased DNA damage repair activity.

Annexins are a structurally homologous family of calcium-dependent phospholipid-binding proteins that includes 12 members (17). Annexins have diverse roles regulating membrane trafficking, cell division, differentiation and apoptosis (18). Moreover, they also function in carcinogenesis (19). Annexin A3 is relatively uncommon and is not as well studied as annexin A1 and A2. Although it has not been extensively studied in NPC cells, annexin A3 has prognostic relevance in prostate cancer (20), lung adenocarcinoma (21) and papillary thyroid cancer (22). Skvortsova *et al* (6) identified annexin A2 and A3 as novel biomarkers in prostate cancer cell lines using two-dimensional difference gel electrophoresis and matrix-assisted laser desorption ionization time-of-flight (TOF)/TOF-mass spectrometry; however, annexin A3 was not verified. In the present study, annexin A3 was first screened as a downregulated protein in the CNE-2R cells, and was also verified using western blot analyses (11). *In vivo* tests showed that annexin A3 expression was significantly lower in the NIR-CNE-2R tumors than in the NIR-CNE-2 tumors. These results suggested that annexin A3 may function in NPC radioresistance. However, its mechanism of action requires further clarification.

The Nm23-H1 protein, encoded by the *Nm23-H1* gene, is a ubiquitously distributed nuclear diphosphate kinase that catalyzes the phosphorylation of nucleoside diphosphates (23). Recently, the 3'-5' exonuclease activity of Nm23-H1 was found to be important for DNA repair, as it maintains genomic stability after ionizing or ultraviolet irradiation (24,25). Kim *et al* (7) found that the overexpression of Nm23-H1, and specifically its nuclear translocation, may be a powerful predictor of radioresistance in head and neck squamous cell carcinoma. These studies suggested that the functional mechanism of Nm23-H1 nuclear translocation may play a role in DNA damage repair, which may affect radioresistance. The present study found that Nm23-H1 protein expression was significantly higher in the CNE-2R cells compared with the CNE-2 cells *in vitro*, as well as being higher in the IR-CNE-2R tumors compared with the IR-CNE-2 tumors. We propose that Nm23-H1 may correlate with DNA damage repair. It is likely that the CNE-2R xenograft tumor cells acquired more DNA damage after irradiation. We hypothesize that this is the reason for the CNE-2R cells obtaining radioresistance.

In conclusion, the present study established a comparable radioresistant and radiosensitive tumor model of human NPC. Furthermore, it was found that abnormal NPM1, annexin A3 and nm23-H1 expression may contribute to NPC radioresistance and thus be potential biomarkers for predicting NPC response to radiotherapy.

Acknowledgements

This study was supported by grants from the National Natural Science Foundation of China (no. 30860329) and the GuangXi Natural Science Foundation of China (no. 0832229).

References

1. Lee AW, Tung SY, Ngan RK, Chappell R, Chua DT, Lu TX, Siu L, Tan T, Chan LK, Ng WT, *et al*: Factors contributing to the efficacy of concurrent-adjuvant chemotherapy for locoregionally advanced nasopharyngeal carcinoma: Combined analyses of NPC-9901 and NPC-9902 Trials. Eur J Cancer 47: 656-666, 2011.
2. Chen Y, Liu MZ, Liang SB, Zong JF, Mao YP, Tang LL, Guo Y, Lin AH, Zeng XF and Ma J: Preliminary results of a prospective randomized trial comparing concurrent chemoradiotherapy plus adjuvant chemotherapy with radiotherapy alone in patients with locoregionally advanced nasopharyngeal carcinoma in endemic regions of china. Int J Radiat Oncol Biol Phys 71: 1356-1364, 2008.
3. Guo Y, Zhu XD, Qu S, Li L, Su F, Li Y, Huang ST and Li DR: Identification of genes involved in radioresistance of nasopharyngeal carcinoma by integrating gene ontology and protein-protein interaction networks. Int J Oncol 40: 85-92, 2012.
4. Feng XP, Yi H, Li MY, Li XH, Yi B, Zhang PF, Li C, Peng F, Tang CE, Li JL, *et al*: Identification of biomarkers for predicting nasopharyngeal carcinoma response to radiotherapy by proteomics. Cancer Res 70: 3450-3462, 2010.
5. Sekhar KR, Reddy YT, Reddy PN, Crooks PA, Venkateswaran A, McDonald WH, Geng L, Sasi S, Van Der Waal RP, Roti JL, *et al*: The novel chemical entity YTR107 inhibits recruitment of nucleophosmin to sites of DNA damage, suppressing repair of DNA double-strand breaks and enhancing radiosensitization. Clin Cancer Res 17: 6490-6499, 2011.
6. Skvortsova I, Skvortsov S, Stasyk T, Raju U, Popper BA, Schiestl B, von Guggenberg E, Neher A, Bonn GK, Huber LA and Lukas P: Intracellular signaling pathways regulating radioresistance of human prostate carcinoma cells. Proteomics 8: 4521-4533, 2008.
7. Kim SH, Lee SY, Park HR, Sung JM, Park AR, Kang S, Kim BG, Choi YP, Kim YB and Cho NH: Nuclear localization of Nm23-H1 in head and neck squamous cell carcinoma is associated with radiation resistance. Cancer 117: 1864-1873, 2011.
8. Li L, Huang S, Zhu X, Zhou Z, Liu Y, Qu S and Guo Y: Identification of radioresistance-associated proteins in human nasopharyngeal carcinoma cell lines by proteomic analysis. Cancer biother Radiopharm 28: 380-384, 2013.
9. Geddes DM: The natural history of lung cancer: A review based on rates of tumour growth. Br J Dis Chest 73: 1-17, 1979.
10. Chang JT, Chan SH, Lin CY, Lin TY, Wang HM, Liao CT, Wang TH, Lee LY and Cheng AJ: Differentially expressed genes in radioresistant nasopharyngeal cancer cells: Gp96 and GDF15. Mol Cancer Ther 6: 2271-2279, 2007.
11. He F, Luo W, Zhang Q, Guo Y, Liu MZ and Ma J: Retrospective analysis of effectiveness of intensity-modulated radiotherapy combined with chemotherapy or not for locoregionally advanced nasopharyngeal carcinoma. Zhonghua Yi Xue Za Zhi 93: 2292-2295, 2013 (In Chinese).
12. Brady SN, Maggi LB Jr, Winkeler CL, Toso EA, Gwinn AS, Pelletier CL and Weber JD: Nucleophosmin protein expression level, but not threonine 198 phosphorylation, is essential in growth and proliferation. Oncogene 28: 3209-3220, 2009.
13. Koike A, Nishikawa H, Wu W, Okada Y, Venkitaraman AR and Ohta T: Recruitment of phosphorylated NPM1 to sites of DNA damage through RNF8-dependent ubiquitin conjugates. Cancer Res 70: 6746-6756, 2010.
14. Derenzini M, Sirri V, Trerè D and Ochs RL: The quantity of nucleolar proteins nucleolin and protein B23 is related to cell doubling time in human cancer cells. Lab Invest 73: 497-502, 1995.
15. Coutinho-Camillo CM, Lourenço SV, Nishimoto IN, Kowalski LP and Soares FA: Nucleophosmin, p53 and Ki-67 expression patterns on an oral squamous cell carcinoma tissue microarray. Hum Pathol 41: 1079-1086, 2010.
16. Grisendi S, Mecucci C, Falini B and Pandolfi PP: Nucleophosmin and cancer. Nat Rev Cancer 6: 493-505, 2006.
17. Gerke V, Creutz CE and Moss SE: Annexins: Linking Ca^{2+} signalling to membrane dynamics. Nat Rev Mol Cell Biol 6: 449-461, 2005.
18. Gerke V and Moss SE: Annexins: From structure to function. Physiol Rev 82: 331-371, 2002.
19. Mussunoor S and Murray GI: The role of annexins in tumour development and progression. J Pathol 216: 131-140, 2008.
20. Kollermann J, Schlomm T, Bang H, Schwall GP, von Eichel-Streiber C, Simon R, Schostak M, Huland H, Berg W, Sauter G, *et al*: Expression and prognostic relevance of annexin A3 in prostate cancer. Eur Urol 54: 1314-1323, 2008.
21. Liu YF, Xiao ZQ, Li MX, Li MY, Zhang PF, Li C, Li F, Chen YH, Yi H, Yao HX and Chen ZC: Quantitative proteome analysis reveals annexin A3 as a novel biomarker in lung adenocarcinoma. J Pathol 217: 54-64, 2009.
22. Jung EJ, Moon HG, Park ST, Cho BI, Lee SM, Jeong CY, Ju YT, Jeong SH, Lee YJ, Choi SK, *et al*: Decreased annexin A3 expression correlates with tumor progression in papillary thyroid cancer. Proteomics Clin Appl 4: 528-537, 2010.
23. Lascu L: The nucleoside diphosphate kinases 1973-2000. J Bioenerg Biomembr 32: 213-214, 2000.
24. Yang M, Jarrett SG, Craven R and Kaetzel DM: YNK1, the yeast homolog of human metastasis suppressor NM23, is required for repair of UV radiation- and etoposide-induced DNA damage. Mutat Res 660: 74-78, 2009.
25. Jarrett SG, Novak M, Dabernat S, Daniel JY, Mellon I, Zhang Q, Harris N, Ciesielski MJ, Fenstermaker RA, Kovacic D, *et al*: Metastasis suppressor NM23-H1 promotes repair of UV-induced DNA damage and suppresses UV-induced melanomagenesis. Cancer Res 72: 133-143, 2012.